Dachev, Ts.P. B.T. Tomov, Yu.N. Matviichuk, R.T. Koleva, J.V. Semkova, V.M. Petrov, V.V. Benghin, Yu.V. Ivanov, V.A. Shurshakov, J. Lemaire, Solar Cycle Variations ff MIR Radiation Environment as Observed by the LIULIN Dosimeter, Radiation Measurements, 30 (3), pp. 269-274, 1999.

SOLAR CYCLE VARIATIONS OF MIR RADIATION ENVIRONMENT AS OBSERVED BY THE LIULIN DOSIMETER

Ts.P. DACHEV*, B.T. TOMOV*, Yu.N. MATVIICHUK*, R.T. KOLEVA*, J.V. SEMKOVA*, V.M. PETROV+, V.V. BENGHIN+, YU.V. IVANOV+, V.A. SHURSHAKOV+, J. F. LEMAIRE#

* Solar-Terrestrial Influences Laboratory, Acad. G. Bonchev St. Block 3, 1113 Sofia, Bulgaria, e-mail: stilrad@bgcict.acad.bg
+ State Scientific Center of Russian Federation, Institute of Biomedical Problems, Khoroshovskoye Sh. 76-a, 123007 Moscow Russia, e-mail: Institute of Biomedical Problems, Russia, shurshakov@mmcc.ibmp.rssi.ru
# Institut d'Aeronomie spatiale de Belgique, Avenue circulaire, 3, 1180 BRUXELLES, Belgique, e-mail: jl@oma.be
Abstract Measurements on board the MIR space station by Bulgarian-Russian dosimeter LIULIN have been used to study the solar cycle variations of the radiation environment. The fixed locations of the instrument in the MIR manned compartment behind 6-15 g/cm^2 of shielding have given homogeneous series of particle fluxes and doses measurements to be collected during the declining phase of 22nd solar cycle between September, 1989 and April, 1994. During the declining phase of 22nd solar cycle the GCR (Galactic Cosmic Rays) flux observed at L > 4 (where L is the McIlwain parameter) has enhanced from 0.6-0.7 (cm^{-2} s^{-1}) up to 1.4-1.6 (cm^{-2} s^{-1}). The long-term observations of the trapped radiation can be summarized as follows: The main maximum of the flux and dose rate is located at the Southeast side of the geomagnetic field minimum of South Atlantic Anomaly (SAA) at L=1.3-1.4. Protons depositing few (nGy cm^2)/particle in the detector predominantly populate this region. At practically the same spatial location and for similar conditions the dose rate rises up from 480 to 1470 μGy/hour dose in silicon in the 1990-1994 time interval, during the declining phase of the solar cycle. On the other hand the flux rises from 35 up to 115 (cm^{-2}. s^{-1}) for the same period of time. A power law dependence was extracted which predicts that when the total neutral density at the altitude of the station decreases from 8.10^{-15} to 6.10^{-16} g/cm^3 the dose increase from about 200 μGy/hour up to 1200 μGy/hour. At the same time the flux increase from about 30 (cm^{-2} s^{-1}) up to 120 (cm^{-2} s^{-1}). The AP8 model predictions give only 5.8% increase of the flux for the same conditions.

EXPERIMENTAL RESULTS

LIULIN experiment description

The dosimeter-radiometer LIULIN was designed for measuring the dose and flux of penetrating particles. It uses a silicon detector with a thickness of 306 microns and area of 2 cm^2. The methods of measurements of the electric output signals of the dosimeter allows us to get simultaneous measurement of the energy absorbed in the detector and the flux of particles passing through it (Dachev et al., 1989). The noise level of the detector and of the electronics is 83 keV. The dose sensitivity of dose measurements is better than 1 nGy/pulse, the overall accuracy being $\pm$ 20%. The statistics obtained during the flight of the instrument on MIR shows that one proton is generating at least 2 pulses in the voltage to frequency converter of the instrument. LIULIN operated on MIR space station between 1989 and 1994. It was placed continuously in the working compartment of MIR space station, which has 6 meters of diameter. The effective mass thickness of shielding of the working compartments is evaluated as 6-15g/cm^2. Thus the main contribution to the count rate measured by LIULIN is likely due to protons and electrons that have energy respectively higher than 100 MeV and 10 MeV outside MIR space station.

Solar cycle variations of the GCR at high values of L as measured with LIULIN

GCR flux distribution during quiet solar and geomagnetic conditions is determined by the Earth magnetic field cut-off, which is energy dependent. The usual distribution measured with LIULIN shows a minimum of 0.1-0.2 (cm^{-2} s^{-1}) close to the magnetic equator and a relative maximum reaching 1-2 (cm^{-2} s^{-1}) at high L values. The dose channel of the LIULIN instrument is unfortunately contaminated by an instrumental noise, which is higher than the measured GCR doses.

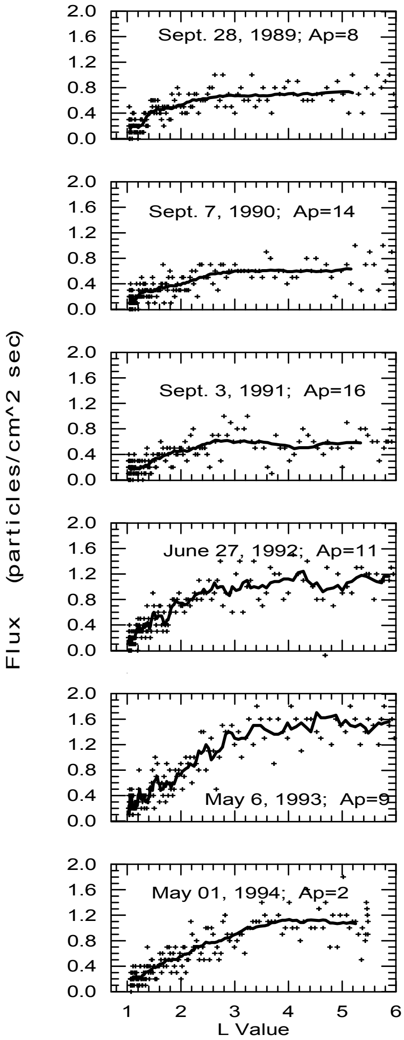

Figure 1. Long term (1989-1994) variations of the GCR flux measured by LIULIN in southern hemisphere. ***Ap*** *is the planetary equivalent daily amplitude. Note the gradual increase of the GCR fluxes at high L value during the declining phase of 22^{nd} solar cycle.*

Available LIULIN GCR flux data for September 28, 1989, September 7, 1990, September 3, 1991, June 27, 1992, May 6, 1993 and May 1, 1994 are presented in Figure 1. The measured fluxes are plotted versus L. The heavy lines correspond to the running average value over 21 independent measurements. Only the values for the

Date	Climax, CO (Counts)	Data from LIULIN			Predicted Dose [2)] (μGy/day)
		Max. Flux (p./cm^2 s)	Aver. Flux (p./cm^2 s)	Dose[1)] (μGy/day)	
28.09.1989	3515.2	1.0	0.630 ± 0.219	69.1	52.0
07.09.1990	3385.4	1.0	0.730 ± 0.174	58.3	44.0
03.09.1991	no data	0.9	0.580 ± 0.170	54.8	48.0
27.06.1992	3836.9	1.5	1.110 ± 0.208	105.3	96.0
06.05.1993	3969.2	2.6	1.530 ± 0.300	145.7	132.0
30.04.1994	4032.0	1.8	1.090 ±0.270	103.0	138.0

Table 1. GCR characteristics at L>4 in the Southern hemisphere. [1)] calculated from fluxes using the model of Hafner, 1971. [2)] by Badhwar et al., 1998.

descending node parts of the orbits in the Southern Hemisphere are shown. The usual trajectory of the station crosses the geographic equator at 30°-60° East longitude. It can be seen that LIULIN GCR flux data have similar L-dependence for all 6 different days shown in Fig. 1. In all cases a "knee" in the data is observed at about L=3.5-4.0. A well-defined increase of the GCR fluxes at high L value is observed during the declining phase of 22nd solar cycle.

The results of the LIULIN as well as Climax Colorado and Badhwar et al., 1997 observations are presented in Table 1. The second column of this table contains the Climax Colorado count rates obtained on the same days as LIULIN data. The third column of the table contains the maximum LIULIN flux for L>4. The fourth column contains the average LIULIN flux for L>4 obtained for 24 to 26 sequential measurements together with the standard deviation of these measurements. The fifth column gives the dose calculated from the LIULIN flux measurements. The flux to dose ratio for 200 MeV protons is used for the calculation based on the Haffner, 1971 method. The intercomparison between the calculated LIULIN doses and those predicted by Badhwar et al., 1997 (sixth column) shows a good agreement.

Solar cycle variations observed in the SAA

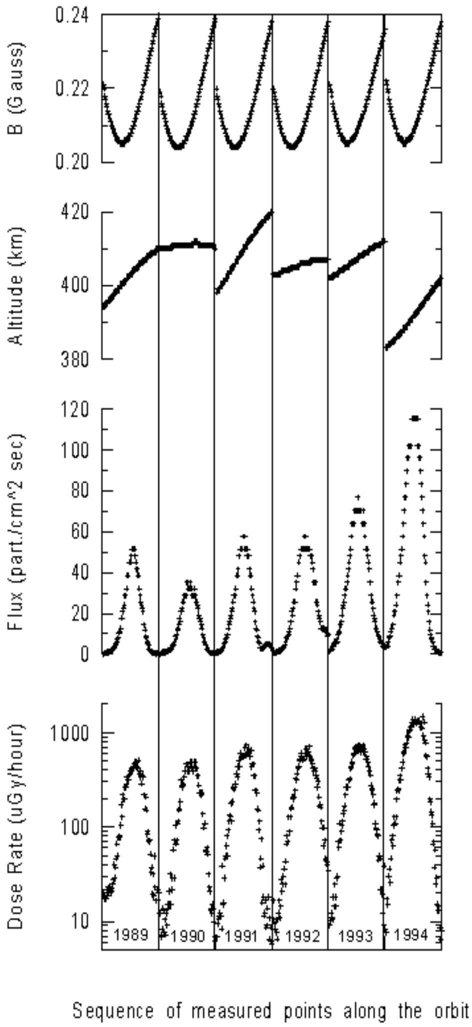

Figure 2. Magnetic field intensity B, the altitude of station, the particle flux and dose rate for 6 crossings of the maximum of the SAA region for declining phase of the solar cycle.

At high latitudes (L>4) the solar cycle variations of the doses measured between 1989 and 1994 are significant. Comparative variations undergo the doses measured in the SAA i.e. at L<2.

LIULIN dose and flux observations versus Universal Time (UT) are shown for six different crossings of the SAA region in the lower panels of Fig. 2. The six different sets of observations were taken for L<2 during six selected days, each of them in a different year, in order to illustrate the long term variation of the maximum dose and flux measured in the SAA for six consecutive years of the solar cycle 22. Chosen were orbits in which MIR space station crosses the SAA along the descending parts of the orbit in order to minimize the influence of the radiation anisotropy, as we do not know the attitude of the station.

These trajectories have been selected so that the orbits pass through the very center of the SAA where the magnetic field intensity B experiences a well defined minimum as illustrated in the top panel of Fig. 2. The minimum value of B for each of these six orbits is almost exactly the same indicating that all these orbits traversed the SAA very close to its center.

The second panel in Fig. 2 shows the altitude of MIR station during these six orbits. The altitudes where B is a minimum are respectively equal to 402 km, 410 km, 410 km, 405 km, 408 km and 390 km. During the 2-nd, 3-rd and 5-th crossings the altitudes where the doses and fluxes reach their maximum values, are nearly equal (408-410 km). In this preliminary survey we could not identify during the years 1989, 1992 and 1994 any orbits passing through the center of the SAA at an altitude closer to 410 km. But a more exhaustive survey will be undertaken later on when the LIULIN database will be finalized in collaboration with the Belgian Institute for Space Aeronomy.

From the bottom panel it can be seen that the maximum value of dose increases year after year from 1989 (when the solar activity was close to its maximum) to 1994 (when solar activity was still in its declining phase).

The peak values of the doses increase gradually with time i.e. with the phase in the solar cycle 22. A non-linear variation is observed after the year 1991 in the peak values of the LIULIN flux measurements. Note that the small secondary peaks in the wings of the 1991 and 1992 flux profiles correspond to the vestiges of the "new" radiation belt which has been formed at L<3 after the Solar Proton Event and geomagnetic storm on March 23 and 24, 1991. For more details please look Mullen et al., 1991 and Dachev et al., 1998.

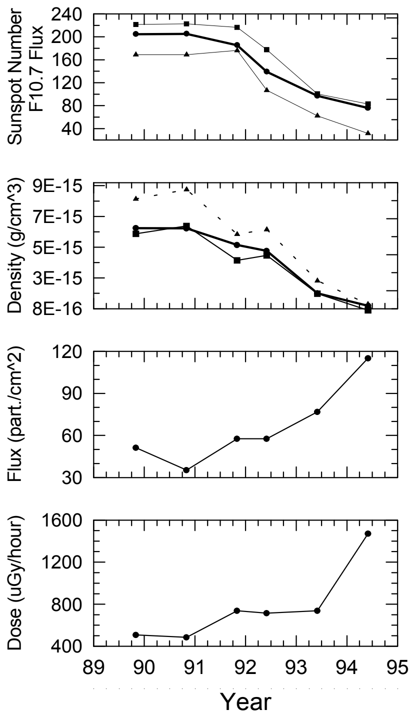

*Figure 3. Same orbits as shown in Fig. 2. The top panel shows the change of the averaged sunspot number for the month before the observations (triangles) as well the value of the F10.7 solar radio flux for the day of observation (dots) and the value of F10.7 averaged over the preceding 30 days (squares)***.** *In the second panel the neutral atmosphere densities calculated using the MSIS-E-90 model are presented: dashed line with triangles represents the densities at 390 km; solid line with squares – the densities at 410 km; and the heavy line with dots shows the densities for the time and place of the dose and flux measurements. In the third and forth panels only the maximum values of flux and dose are shown*

In the two lower panels of Fig. 3 we plotted the maximum values of the fluxes and doses versus time in the solar cycle 22. The atmospheric densities (in g/sm^3) at 410 km, 390 km and at the actual altitude of the MIR station in the SAA, for the day and UT corresponding to the observations, calculated using the Mass-Spectrometer– Incoherent -Scatter (MSIS-E-90) model Bilitza, 1997b are displayed in the second panel of Fig. 3. The top panel shows the change of the solar activity indexes needed to determine the atmospheric density - averaged sunspot number for the month before the observations, the value of the F10.7 solar radio flux for the day of observation and the value of F10.7 averaged over the preceding 30 days. It can be seen that the calculated densities at 410 km, 390 km and at the actual altitude of the MIR station decrease with time in parallel with the solar activity indexes shown in the panel above. This is expected since the atmospheric density in the upper atmosphere is determined by the rate of heating of the thermosphere by the UV and EUV solar radiation which varies in parallel with the radio flux (F10.7 cm) emitted by the Sun.

During the maximum of solar activity the temperature of the upper atmosphere is large and the neutral density reaches a maximum of about 6.10^{-15} g/cm^3 at the altitude of the MIR station (about 410 km altitude). The mass of atmosphere deflecting and absorbing the trapped particles above this altitude is at maximum. As a consequence, the flux of the energetic particles, which mirror at or below the MIR station, is then smaller than during periods of minimum solar activity when the density at the same altitude is reduced to values of the order of 1.10^{-15} g/cm^3.

Fig.3 nicely illustrates how the reduction of the atmospheric density due to the diminishing solar activity leads to the long-term enhancement of the maximum dose and particle flux in the SAA. These results are shown in Table 2. The first column gives the date and UT of the LIULIN observation corresponding to the maximum dose given in column 2; the third column gives the integrated dose also given in Fig. 2; the third column gives the atmospheric density at the altitude of the MIR station; the next column gives the measured maximum particle flux in (cm^{-2} s^{-1}); the last column gives the corresponding fluxes of protons with energies larger then 100

MeV as predicted at this altitude by the AP-8 empirical model (Bilitza,1977). These model values have been obtained with the latest version of the UNIRAD software package developed by Heynderickx et al., 1996 for ESA at the Belgian Institute for Space Aeronomy.

It can be seen that the values predicted by AP-8 model for solar maximum in the first three rows corresponding to the years 1989 - 1991, are 5.8% lower then those predicted by this same model for solar minimum in the last three rows of Table 2 corresponding to the years 1992 - 1994. This solar cycle change can be compared to that obtained from the LIULIN observations. From Table 2 it can be seen that the maximum flux observed with LIULIN changes by a factor of 200% between 1989 and 1991 which is a much larger change than that predicted by the AP-8 model.

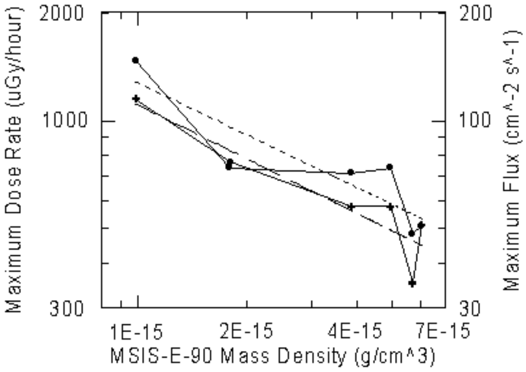

Figure 4. Dose and flux dependence by the neutral density at the altitude of the station. The line with crosses corresponds to the maximum fluxes (right scale); the line with dots corresponds to the maximum value of the dose rate (left scale). The dashed line corresponds to a power law fit of the maximum dose rate, while the long dashed line corresponds to a power law fit of the maximum flux.

Figure 4 illustrates the anti-correlation between the maximum doses and fluxes, and the density taken from Fig. 3. The neutral atmospheric density at the altitude of the MIR station has been obtained by the MSIS-E-90 model using Bilitza, 1997 b. Presented are the maximum fluxes, the maximum values of the dose rates and their power law fits, obtained by the method of fitting. These power law approximations relating the measured maximum dose rate and flux and the neutral atmospheric density are given by:

$$(\text{Dose rate}) = 0.000068258*(\text{Neutral Density})^{-0.484742}$$

$$(\text{Flux}) = 0.00000322849*(\text{Neutral Density})^{-0.502316}$$

Where (Neutral Density) is in g/cm^3 and the (Dose rate) is in µGy/hours and (Flux) is in (cm^{-2} s^{-1}).

Date	LIULIN Max. Dose (µGy/hour)	MSIS Density (g/cm^3)	LIULIN Max. ux (cm^2 sec^{-1})	AP-8>100 MeV [1)] (part./cm^2 sec)
29.09.1989	507	6.041E-15	51.2	
06.09.1990	484	5.685E-15	35.2	
12.09.1991	737	4.944E-15	57.6	1.046E+04
27.04.1992	714	4.556E-15	57.6	
08.05.1993	737	1.794E-15	76.8	
30.04.1994	1470	9.898E-16	115.2	1.107E+04

Tabulated data for the declining phase of the solar cycle

Note that the coefficients in this equation are only valid for the altitude of the MIR station when it is at 410 km altitude.

CONCLUSIONS

We have confirmed a well-defined increase of the Galactic Cosmic Ray (GCR) flux at L>4 during the decline of solar cycle 22. The GCR flux increased from an average value of 0.58 part/cm^{2}sec in 1991 up to 1.53 (cm^{-2} s^{-1}) in 1993.

The peak value of the dose rate and flux of particles measured by LIULIN in the SAA increase gradually by a factor of 200% between 1991 and 1994 at the altitude of 410 km. This increase is much larger than that predicted at this same altitude by the AP-8 model between solar maximum and solar minimum activity. This increase is attributed to the decrease of the atmospheric density in the layers above the MIR station during the declining phase of solar activity. It is due to the lower rate of heating of the upper atmosphere when the solar UV and EUV radiation diminishes during the solar cycle. A power law relationship has been deduced between local atmospheric density at the altitude of MIR station and the maximum dose rate in the center of the SAA when the neutral density decreased from 8.10^{-15} g/cm^3 to 6.10^{-16} g/cm^3, the maximum dose increases from 200 uGy/hour to 1200 uGy/hour, while the flux of particles increased from 30 (cm^{-2} s^{-1}) to 120 (cm^{-2} s^{-1}).

ACKNOWLEDGEMENTS

Bulgarian team and J.L. gratefully acknowledge support from the Belgium Institute for Space Aeronomy, Brussels under an Agreement for execution of a joint Bulgarian-Belgian research project.

REFERENCES

Dachev, Ts. P., Yu.N. Matviichuk, J.V. Semkova, R.T. Koleva, B. Boichev, P. Baynov, N.A. Kanchev, P. Lakov, Ya.J. Ivanov, B.T. Tomov, V.M. Petrov, V.I. Redko, V.I. Kojarinov and R. Tykva (1989) Space radiation dosimetry with active detection's for the scientific program of the second Bulgarian cosmonaut on board the MIR space station. Adv. Space Res., 9, 10, 247.

Badhwar, G.D., V.A. Shurshakov and V.V. Tsetlin (1997) Solar modulation of dose rate onboard the MIR space station. IEE Trans. on Nucl. Sci., 44, No 6, 2529.

Haffner, J.W. (1971) Nuclear radiation and protection in space. 114, Moscow, Atomizdat,. (In Russian).

Mullen, E.G., M.S. Gussenhoven, K. Ray and M. Violet (1991), A double-peaked inner radiation belt: cause and effect as seen on CRRES, IEEE Transactions of Nuclear Science, V. 38, No 6, 1713.

Dachev Ts.P., J.V.Semkova, Yu.N.Matviichuk, B.T. Tomov, R.T. Koleva,, P.T. Baynov, V.M. Petrov, V.V. Shurshakov, Yu. Ivanov (1998) Inner Magnetosphere Variations after Solar Proton Events. Observations on Mir Space Station In 1989-1994 Time Period, Adv. Space Reas., 22, No 4, 521.

Bilitza, D. (1997a) AE-8/AP-8 Radiation Belt Models. http://nssdc.gsfc.nasa.gov/space/model /models/trap.html, September, 1997a.

Bilitza, D. (1997b) MSIS-E-90 Atmosphere Model. http://nssdc.gsfc.nasa.gov/space/model /models/msis.html, September, 1997b.

Heynderickx, D., M. Kruglanski and J. Lemaire (1996) UNIRAD User Manual, BIRA/IASB, November 1996.